HHS Public Access

Author manuscript

Gene Expr Patterns. Author manuscript; available in PMC 2016 March 26.

Published in final edited form as:

Gene Expr Patterns. 2015 March ; 17(2): 98–106. doi:10.1016/j.gep.2015.03.002.

Anillin localization suggests distinct mechanisms of division plane specification in mouse oogenic meiosis I and II

Bedra Sharif[1], **Tanner Fadero**[2], and **Amy Shaub Maddox**[2]

[1]Institute for Research in Immunology and Cancer, Université de Montréal, Montréal, Québec, Canada

[2]Department of Biology, University of North Carolina, Chapel Hill, NC, USA

Abstract

Anillin is a conserved cytokinetic ring protein implicated in actomyosin cytoskeletal organization and cytoskeletal-membrane linkage. Here we explored anillin localization in the highly asymmetric divisions of the mouse oocyte that lead to the extrusion of two polar bodies. The purposes of polar body extrusion are to reduce the chromosome complement within the egg to haploid, and to retain the majority of the egg cytoplasm for embryonic development. Anillin's proposed roles in cytokinetic ring organization suggest that it plays important roles in achieving this asymmetric division. We report that during meiotic maturation, anillin mRNA is expressed and protein levels steadily rise. In meiosis I, anillin localizes to a cortical cap overlying metaphase I spindles, and a broad ring over anaphase spindles that are perpendicular to the cortex. Anillin is excluded from the cortex of the prospective first polar body, and highly enriched in the cytokinetic ring that severs the polar body from the oocyte. In meiosis II, anillin is enriched in a cortical stripe precisely coincident with and overlying the meiotic spindle midzone. These results suggest a model in which this cortical structure contributes to spindle re-alignment in meiosis II. Thus, localization of anillin as a conserved cytokinetic ring marker illustrates that the geometry of the cytokinetic ring is distinct between the two oogenic meiotic cytokineses in mammals.

Keywords

meiosis; cytokinesis; anillin; oocyte maturation

Introduction

Cytokinesis is the physical partitioning of two daughter cells. Cell shape change, or furrowing, during cytokinesis is accomplished by a transient structure called the cytokinetic ring, which is rich in actin filaments, non-muscle myosin II and many other cytoskeletal

Correspondence to: ASM; 919-843-3228, asm@unc.edu.

proteins. The placement and activation of the cytokinetic ring are determined by the geometry of the anaphase spindle (Argiros et al., 2012; Bringmann, 2008; von Dassow et al., 2009). In various cell types, bundled and antiparallel microtubules of the spindle midzone, and equatorial astral microtubules, have been implicated in specifying the overlying cortex as the cell equator, or division plane (reviewed by Green et al., 2012). Anaphase spindle signalling converges on the activation of the small GTPase RhoA. RhoA elicits cytokinetic ring assembly by activating Diaphanous family formins to stimulate growth of long, unbranched actin filaments, and several kinases that in turn activate non-muscle myosin II. The cytokinetic ring forms a belt around the cell equator and constricts, drawing the plasma membrane with it, progressively closing off the cytoplasmic connection between the daughter cells.

Anillin, a conserved multi-domain protein, is another RhoA effector, as it becomes highly enriched at the cell equator in a Rho-dependent manner (reviewed by Piekny and Maddox, 2010). Distinct domains within the N-terminus of anillin can bind active myosin and bundle actin filaments (Field et al., 1995; Straight et al., 2003). At its C-terminus, anillin has an anillin homology domain (AHD) and a pleckstrin homology (PH) domain that bind the cytokinesis master regulator RhoA, plasma membrane lipids and the septins (Kinoshita et al., 2002; Liu et al., 2012; Piekny and Glotzer, 2008; Oegema et al., 2000). The septins form hetero-oligomeric complexes that assemble into filaments (Lukoyanova et al., 2008), rings and gauzes (Fung et al., 2014). In cytokinesis, septins may link the plasma membrane to the actin cytoskeleton (Fung et al., 2014; Mostowy and Cossart, 2012). Anillin localizes to the nucleus in interphase in most species. Metaphase localization varies among cell types: anillin is diffusely cytoplasmic in mammalian and nematode mitotic cells, globally cortical in mitotic *Drosophila* cultured cells, and cortically encircling the nucleus or spindle in the *Drosophila* blastoderm and *C. elegans* oogenic meiosis (Piekny and Maddox, 2010). Anillin enriches prominently at the cytokinetic furrow in anaphase, and at the midbody ring at the end of cytokinesis (Field and Alberts, 1995; Kechad et al., 2012). Anillin is also highly enriched in the stable ring canals of egg chamber nurse cells, spermatocytes, and the embryonic blastoderm in *Drosophila* (Field et al., 2005; Giansanti et al., 1999).

The primary function of anillin during cytokinesis has remained elusive, despite its importance in preventing cytokinesis failure and binucleation. In mammalian and *Drosophila* cultured cells, anillin depletion results in oscillation of the furrow along the interpolar axis and eventual regression. This may reflect a role in anchoring the contractile apparatus to the spindle (D'Avino et al., 2008; Frenette et al., 2012; Gregory et al., 2008; Hickson and O'Farrell, 2008; Liu et al., 2012; Piekny and Glotzer, 2008). In *Drosophila* cultured cells, anillin is required for the stable closure of the midbody, an activity dependent on the anillin homology and PH domains (thought to bind septins and plasma membrane lipids). These results suggest that anillin's capacity to link the actomyosin cytoskeleton to the plasma membrane is essential for midbody stability and avoidance of binucleation (Kechad et al., 2012). In the *C. elegans* zygote, anillin is not necessary for mitotic cytokinesis, but is required for the meiotic cytokineses that separate the polar bodies from the oocyte. The meiotic cytokinetic rings begin as discs and transform, in an anillin-dependent manner, into a stack or coil of actomyosin rings (Dorn et al., 2010). Thus, anillin

has been implicated in cortex-spindle linkage, cortex-membrane linkage, and actin organization.

Polar bodies are the daughter cell products of the highly asymmetric cell divisions during oogenesis. The asymmetry of this division is important for production of oocytes sufficiently large to support early embryonic development, and is achieved by eccentric placement of the meiotic spindle. The association between the spindle and the cortex, initially to displace the spindle from the center of the cell and later to anchor it at the cortex, is mediated by a cytoplasmic meshwork of actin nucleated by Formin 2 (Azoury et al., 2008; Leader et al., 2002; Schuh and Ellenberg, 2008). The spindle, in turn, triggers the differentiation of the adjacent cortex (Chaigne et al., 2012) such that it is free of microvilli and cortical granules and possesses a cortical actin cap that is surrounded by a ring of myosin (Ducibella et al., 1990; Longo and Chen, 1985). PAR polarity proteins, the small GTPases Rac and Cdc42, and the Arp2/3 complex are implicated in this cortical polarization (Dehapiot et al., 2013; Duncan et al., 2005; Halet and Carroll, 2007; Na and Zernicka-Goetz, 2006; Vinot et al., 2004; Yi et al., 2011; Yi and Li, 2012). Upon anaphase of meiosis I, one mass of segregated chromatin extends into a protrusion from the oocyte surface and is cleaved from the oocyte by the actomyosin cytokinetic ring. Upon its formation near the cortex, the metaphase II spindle lies with its long axis parallel to the oocyte surface, with both spindle poles and the chromosomes proximal to cortex. Via the small GTPase Ran, chromatin near the egg cortex elicits the formation of an actin cap surrounded by a myosin II ring (Deng et al., 2007; Wang et al., 2011). In anaphase, the spindle becomes perpendicular with the cortex and one mass of segregated chromatin is partitioned into the second polar body.

To date, the localization of anillin and the possibility of a conserved function in cytoskeletal organization during mammalian oogenesis have not been examined. Here, we establish the expression and localization of anillin during the meiotic divisions of mouse oocytes. Anillin mRNA and protein are present in meiosis and become more abundant during metaphase. Anillin localizes to the actin cap over the metaphase I spindle and to the cytokinetic ring during anaphase of meiosis I and II. Our observations indicate that furrow specification occurs via distinct mechanisms between the two meiotic divisions. In meiosis I, the anaphase spindle is perpendicular to the cortex, and anillin and other components of the cytokinetic ring encircle the nascent polar body. In anaphase of meiosis II, when the spindle is parallel to the cortex, anillin and actin enrich in a line circumscribing the spindle midzone. At apparently later anaphase timepoints, this structure appears to have ingressed asymmetrically against the spindle. This apparent sequence of events suggests that the meiotic cytokinetic ring contributes to physically reorienting the meiosis II spindle so that it becomes perpendicular to the cortex during second polar body emission. Thus, whereas in meiosis I the circumferential ring closes inward on the extruded anaphase spindle midzone, in meiosis II, an initially asymmetric cytokinetic structure transforms into a circumferential ring only after spindle reorientation.

Results and Discussion

Anillin mRNA and protein are expressed during meiotic maturation of the mouse oocyte

Anillin is required for proper maternal meiotic cytokinesis in *C. elegans*, but anillin has never been examined during the asymmetric meiotic oocyte/polar body divisions of the mammalian oocyte. To study the involvement of anillin in mammalian meiotic divisions, we first tested anillin expression at the mRNA and protein level during meiotic maturation of the mouse oocyte. We isolated mouse oocytes at the germinal vesicle (GV) stage directly from the ovaries of unstimulated (non-super ovulated) female mice, and obtained oocytes soon after germinal vesicle (nuclear envelope) breakdown (GVB), later in meiosis I and in meiosis II by culturing them according to standard methods (Figure 1A; Behringer, 2014). We prepared mRNA from 50 cells at each stage and used poly-dT primers to make total cDNA in a reverse transcription reaction. The cDNA was then probed for the expression of our genes of interest with a SYBR Green PCR assay and gene specific primers. Anillin is expressed throughout meiotic maturation. Anillin mRNA levels increased slightly from GV to late metaphase I, and then decreased slightly in metaphase II (Figure 1B). These results support the idea that anillin plays a role in mammalian oogenic meiosis I and II.

To place our anillin expression data in the context of transcriptional regulation of other cytoskeletal proteins, we examined mRNA levels for two isoforms of the actin crosslinker α-actinin (Fung et al., 2014; Kinoshita et al., 2002), and septins 2 and 7, which form part of a hetero-oligomer that assembles into plasma membrane-associated filaments and sheets (Fung et al., 2014; Mostowy and Cossart, 2012), all of which have been implicated in cytokinesis. Septin 7 and α -actinin 1 and 4 transcript levels dropped significantly in metaphase II compared with earlier stages, while septin 2 mRNA levels almost doubled in meiosis II (Figure 1B). Our results suggest that mRNAs of anillin and septin 2 are stabilized, while those of septin 7 and the α–actinins are degraded, as has been observed for some mRNAs during mouse meiotic maturation (Su et al., 2007).

To examine whether anillin protein is present in mouse oocytes, we used three antibodies for Western blotting. We first tested whether these antibodies recognized a band corresponding to anillin in extracts of the mouse cell line, NIH3T3. The three anillin antibodies detected a prominent band migrating at ∼180 KDa, as expected (Figure 1E; Oegema et al., 2000). All three antibodies also recognized a second band migrating at ∼110 KDa, which may correspond to a splice form or proteolytic product (Figure 1E). Interestingly, only the slower-migrating band was detected in oocytes (Figure 1C). Anillin protein was undetectable in GV-stage oocytes and its levels steadily rose from GVB to metaphase of meiosis II. This result suggests that anillin acts late in egg maturation. To control for extract loading, we used the same number of oocytes per lane of gel (n=50 oocytes), and also probed the same blot for other cytoskeletal proteins. Unlike anillin, myosin II and actin are most abundant at the GV stage, before meiotic resumption, and their abundance decreases after the completion of meiotic maturation at MII stage (Figure 1C, D). Actin transcript levels have been observed to decrease in this manner during meiotic maturation of human oocytes (Steuerwald et al., 2001). Tubulin protein levels fluctuate during meiosis I, increasing at GVB and MI stages, and then decreasing in MII (Figure 1C, D), as has been

observed (Azoury et al., 2011). Thus, anillin transcript and protein are present during meiotic maturation of the mouse oocyte.

Anillin, septin 11, and F-actin enrich in the polar oocyte cortex throughout meiosis I

Anillin is required for various aspects of cytokinesis across phylogeny (Hickson and O'Farrell, 2008; D'Avino, 2009; Piekny and Maddox, 2010), but its exact roles in contractile ring function are still debated. The asymmetric cytokinetic events that partition the small polar bodies from the larger oocyte can be thought of a sensitized system with additional molecular and physical requirements, compared with mitosis (Dorn et al., 2010), and thus may reveal general principles of cytokinesis that are masked when more redundancies are present. We next investigated the localization of anillin during mouse meiosis I and II. We first tested our antibody, raised against mouse anillin, by immunofluorescence staining of the mouse cell line NIH3T3. As expected (Oegema et al 2000), anillin localized to the nucleus in interphase, the cytoplasm in prometaphase and metaphase, an equatorial band in anaphase, and the midbody in telophase (Figure 1E).

We then fixed and stained mouse oocytes undergoing meiosis I and examined anillin localization. In late metaphase I, anillin localized to the cortex overlying the meiotic spindle (Figure 2A). This was the case whether the spindle was parallel or perpendicular to the cortex (Figure 2A). This localization was distinct from that seen in NIH3T3 cells or the *C. elegans* zygote, in which anillin does not localize to the cortex in metaphase (Maddox et al., 2005), but in agreement with observations of the metaphase actin cap in meiosis I and II (Maddox et al., 2012).

To acquire oocytes undergoing first meiotic cytokinesis, oocytes harvested in GV stage (prophase I) were cultured until the appearance of a protruding polar body, and immediately fixed. Oocytes were then stained with antibodies against anillin and tubulin, and DAPI. Separate oocytes were stained with Phalloidin to label F-actin. Anillin was highly enriched in the oocyte cortex at the base of the nascent polar body (Figure 2A) and excluded from the cortex toward the tip of the polar body (Figure 2A). In oocytes that were fixed as the first polar body is becoming severed from the oocyte, anillin was enriched in a constricted ring at the neck connecting the polar body and oocyte (Figure 2A; summarized in Figure 2B). The pattern of localization of anillin was distinct from that of F-actin, which localizes over the entire protrusion (Figure 2C). These results suggest that anillin is enriched in the unbranched F-actin-rich contractile ring and excluded from the differentially regulated zone of dynamic F-actin on the nascent polar body (Maddox et al., 2012). In some cells, multiple, stacked rings were present as previously observed (see Figure 2E; Dorn et al 2010). These results support the idea that anillin contributes to the conversion of an initially flat cytokinetic disc into a coil or stack during polar body cytokinesis. These results also demonstrate that anillin becomes more highly enriched at the actin cap and cytokinetic ring as meiosis I proceeds (Figure 2A′), whereas F-actin enrichment in the region of the spindle is relatively stable (Figure 2C′).

To carry out its functions in the contractile rings of *Drosophila* and *C. elegans*, anillin is thought to function with the septins. To explore whether anillin acts with septins in mouse polar body cytokinesis, we stained oocytes with an antibody specific to septin 11 (Huang et

al., 2008), which is implicated in cytokinesis in human cultured cells (Estey et al., 2010). Interestingly, septin 11 localized to the apical surface of the prospective polar body (Figure 2D, asterisk) and not the furrowing region in early anaphase (Figure 2D, arrowhead). It remained somewhat enriched on the distal polar body cortex as cytokinesis proceeded, but did become enriched in the neck region after substantial constriction had occurred (Figure 2D, arrow). These results suggest that anillin and septin work together in a subset of cytokinetic events, specifically late in ring closure, when they could anchor the contractile ring to the plasma membrane and prevent the polar body from receiving excess surface area, as has been suggested (Dorn et al., 2010).

Anillin and actin form an asymmetric curvilinear structure over the meiosis II spindle midzone

After emission of the first polar body, the now univalent chromosomes condense and align on a second meiotic spindle that assembles close to the first polar body. We next examined anillin localization during anaphase of meiosis II. To obtain oocytes in anaphase of meiosis II, we harvested eggs in metaphase II 18-20 hours after the administration of human chorionic gonadotropin (hCG) to female mice and artificially activated the collected eggs with hyaluronidase.

Unlike the meiosis I spindle, which is often perpendicular to the cortex, the meiosis II spindle is usually parallel with the overlying cortex in metaphase and becomes perpendicular to the cortex in anaphase (Cowan, 2007). It is not known how or when in meiosis II spindle rotation occurs. It has been proposed that a cortical invagination towards the meiosis II spindle midzone re-aligns the spindle, which subsequently elicits formation of a distinct circumferential cytokinetic ring (Wang et al., 2011).

Indeed, in oocytes in anaphase of meiosis II, the spindle was still parallel to the cortex. In these early anaphase II cells, anillin was strongly enriched in a linear domain precisely co-incident with the middle of the meiotic anaphase spindle midzone where exclusion of the anti-tubulin antibody suggests that the tightest bundles of antiparallel microtubules are present (Figure 3A top row). Co-localizing with anillin were paired bundles of F-actin (Figure 3A). These results suggest that the spindle midzone and associated protein complexes elicit the formation of this F-actin- and anillin-rich structure, as is the case in mitosis.

In anaphase II cells with the spindle perpendicular to the cortex and a larger connection between the egg and polar body, anillin, F-actin, and myosin localized to a partial ring at the midzone (Figure 3A middle row, Figure 3B arrow). In more advanced anaphase II cells, anillin and F-actin occupy a fully circular ring around the meiotic spindle midzone (Figure 3A bottom row). Interestingly, but in agreement with published findings, the mature and constricted ring does not appear enriched for myosin IIA, suggesting that it plays a less prominent role than myosin IIB in late meiotic cytokinesis (Figure 3C top row; Simerly et al., 1998). Collectively, these results demonstrate the existence of an asymmetric, linear, midzone-associated cytokinetic structure enriched for anillin and actin. This structure increases in curvature concurrent with spindle realignment, and likely transforms into the circular cytokinetic ring observed in late meiosis II. Our results also suggest that, as in

mitosis, the meiosis II spindle midzone plays a pivotal role in specifying the cytokinetic cytoskeleton. Finally, association between this cortical partial ring and the meiotic spindle midzone, together with contraction of the cortical feature, may re-align the meiosis II spindle, while completing the asymmetric cytokinesis of the second polar body (Figure 4). This latter interpretation resembles that of Deng and colleagues (Wang et al., 2011), except that they presume that the asymmetric structure and circumferential ring are distinct structures. Future work will involve live imaging of fluorescently tagged probes for anillin, F-actin or myosin to determine whether the asymmetric actomyosin arc and the cytokinetic ring represent the same object throughout maturation, or are indeed separate structures.

Materials and Methods

Animals

Female mice (C57BL/6 × CBA) F1 were purchased from The Jackson Laboratory at age 4 weeks and housed in ventilated cages where the temperature of the room was set to 22°C ±2°C, with relative humidity between 45-55% and light: dark cycle of 12h:12h. The females were euthanized by CO_2 gassing, according to the guidelines of the Canadian Council for Animal Care (CCAC). Super-ovulations were carried out to improve the yield of mouse eggs at the MII stage. To do so, the mice were given a single IP injection of PMSG (5 IU/0.1 ml), followed by a single IP injection of hCG (5 IU/0.1 ml) 48 hrs later. Super-ovulated females were euthanized 12-20 hours post hCG for the isolation of eggs in various stages of MII.

Oocyte Isolation and Culture

Isolated ovaries were placed in M2 medium (Sigma) containing 10μM Milrinone (Sigma) to maintain GV stage arrest. Oocytes were isolated then cultured in M16 medium as described previously (Behringer, 2014; Na and Zernicka-Goetz, 2006) in a humidified incubator with 5% CO2, at 37°C. GV stage oocytes were collected after a recovery period of about 30 min in culture. GVB (or GVBD) oocytes were collected 2 hrs after culture in M16, while late MI oocytes were collected 7-8 hrs after GVB. MII stage oocytes were collected 12-14 hours after hCG injection. MII oocytes were isolated from the ampullae of oviducts and placed into M2 medium supplemented with 200 IU/ml of hyaluronidase (Sigma) to remove cumulus cells. MII oocytes were then cultured in M16 medium, in the incubator, for 30 min to recover before further processing.

Cell Culture

Murine NIH3T3 cells were cultured in DMEM medium (Gibco/life technologies) supplemented with 10% FBS at 37°C with 5% CO_2.

RNA Extraction

For RNA extracted from mouse oocytes, approximately 50 oocytes at each stage of maturation (GV, GVB, MI, and MII) were collected directly into 1.5 ml microfuge tubes with minimal M16 medium. The RNA was extracted using the PicoPure RNA Isolation Kit (ARCTURUS/Applied Biosystems/ life technologies) according to the manufacturer's instructions. The RNA was eluted in 12 μl nuclease-free water (Ambion/life technologies).

The elution was then treated with DNAse using the DNA-Free DNAse Treatment and Removal Kit (Ambion/ life technologies) in the following reaction: 8.5 µl RNA extract, 0.5 µl DNase I, and 1 µl 10× buffer. Steps were followed according to the manufacturer's instructions. The volume of the supernatant was measured with P20 pipette and made up to exactly 11 µl with nuclease-free water, then stored at -80°C until reverse transcription and cDNA synthesis.

cDNA Synthesis

For RNA isolated from mouse oocytes, Superscript III Reverse Transcriptase (Invitrogen/ Life Technologies) was used for the reverse transcription in 20 µl reaction volume according to manufacturer's instructions. Briefly, 1 µl 10 mM dNTP Mix (Invitrogen, life technologies) and 1 µl oligo (dT)20 primer at 0.5 µg/µl was added to 11 µl RNA and incubated at 65°C for 5-7 min to denature the double stranded RNA, then the RNA was put on ice to cool the contents of the reaction and keep the denatured state. The Reverse Transcription master mix was prepared as follows: 4 µl 5× first strand buffer, 1 µl 0.1 M DTT, 1 µl RNaseOUT (Invitrogen/Life Technologies) and 1 µl SuperScript III enzyme. The 7 µl of master mix was added to 13 µl of denatured RNA and the reaction was incubated at 50°C for 1 hr. The SuperScript III enzyme was heat inactivated at 70°C for 15 min, and the cDNA was stored at -20°C.

Primers

The cDNA sequences of our genes of interest (see Table 1) were obtained from PubMed nucleotide (http://www.ncbi.nlm.nih.gov/pubmed/). If more than one sequence variant was found, the sequences of the ORF were aligned and checked. Primers were designed using Primer3 Input (http://bioinfo.ut.ee/primer3-0.4.0/) to a sequence in common to all sequence variants for each gene. All primers were designed to amplify 100bp-200bp regions within the ORF for each gene of interest. For primer sequences, see Table 1. All primers were diluted with water to 10 µM working solution before use in PCR amplifications.

Quantitative Real Time-PCR

Mouse oocyte cDNA was diluted 1 in 5 by taking 6 µl cDNA and adding 24 µl nuclease-free water. This was done for each sample of oocyte cDNA (GV, GVB, MI and MII). Primers, SYBR Green master mixes and the Real Time-PCR was performed as follows: the primers were prepared by mixing 1 µl forward primer with 1 µl reverse primer to make a 2 µl oligo mix at 50 µM each. This was done for all the primer pairs listed in the Table 1. Then a SYBR Green master mix was prepared, using the PerfeCTa SYBR Green FastMix (Quanta Biosciences) as follows: 2× SYBR FastMix (5 µl), mixed oligos (0.05 µl), and water (3.45 µl) per single reaction. The master mix volumes were adjusted depending on the number of reactions per primer pair, and a separate master mix was assembled for each primer pair. Then the template cDNA (1.5 µl) was added to each of the designated wells of a 384-well plate with an electronic pipette, except for the wells designated for non-template control (NTC) where water was added instead. The plate was centrifuged for 20-30 seconds at 3,000 rpm to bring the drops of pipetted template cDNA to the bottom. Then 8.5 µl of master mix was added to each well, bringing the total volume in each reaction well to 10 µl. The plate was centrifuged again, then sealed with adhesive film. The plate was then loaded onto an

ABI PRISM 7900HT, and the fast PCR program was run: 50°C for 2 min, then 40 cycles of 95°C for 3 min, 95°C for 5 sec, 60°C for 30 sec. The program was set up to include a Dissociation or Melt Curve cycle at the end of PCR cycling to make sure that only a single product was amplified in each sample reaction.

Western Blotting

NIH3T3 Cells—To prepare protein extract from NIH3T3, the cells were grown in 10 cm culture dish until confluence. The culture media was carefully removed, and the cells washed twice with cold PBS. Cold RIPA Buffer (Sigma)(1 ml) was added to the washed cells, and the cells were incubated on ice for 5 minutes, swirling the plate occasionally for uniform spreading. The lysate was gathered to one side using a cell scraper and collected into a clean 1.5 ml microfuge tube. The sample was centrifuged at 14,000 × g (∼12,000 rpm) for 15 min to pellet the cell debris. The supernatant was transferred to a new microfuge tube, and then divided into 200 µl aliquots, to which 100 µl 4× Sample Buffer was added. All the resulting samples were heated to 100°C for 5 min, under the fume hood. The denatured extract was stored at -80°C until loading onto SDS-PAGE gels. In the first blot to test different anillin antibodies, 7 µl and 15 µl extract was loaded per lane. In subsequent blots, when using the NIH3T3 extract as a positive control, 15 µl extract was loaded per lane.

Mouse Oocytes—Mouse oocytes were collected directly into a 1.5 ml microfuge tube containing 5 µl 4× Sample Buffer. The oocytes were first washed in pre-warmed M2 medium diluted with PBS (1:50) in order to reduce BSA content of the sample. The oocytes were collected at different stages of meiotic maturation (GV, GVB, MI and MII) as described above. The volume of the oocyte/Sample Buffer extract was measured with a pipette, and more 1× Sample Buffer was added to equalise the volumes in all samples (no more than 20 µl). The samples were heated to 100°C for 5 min and then cooled on ice, before loading onto an SDS-PAGE gel. About 50 oocytes were loaded per lane. The Prestained SDS-PAGE standards (Bio-Rad) were also loaded (10 µl) for size control.

SDS-PAGE was performed using the Mini-PROTEAN Tetra Cell system (Bio-Rad) and the gel was transferred to nitrocellulose. Ponceau S was used to verify the efficient transfer of proteins. The membrane was blocked (5% milk in TBS+0.1% Tween) for 1 hr at RT, and then incubated with the primary antibody diluted in block for 1-2 hrs at RT (or overnight at 4°C), washed in 3×10 min changes in block, incubated with the HRP-conjugated secondary antibody diluted in block for 1-2 hrs at RT, rinsed in 3×10 min changes in TBS+0.1% Tween, incubated with ECL reagent (Western Lightning Plus-ECL) for 1 min, and then exposed to film (Kodak) that was processed by an film developer.

To re-blot the same membrane with a different set of antibodies, the membrane was washed in TBS+0.1% Tween, and then incubated in block plus 1% sodium azide (Sigma). The membrane was then rinsed in block without sodium azide and processed for immunoblotting as described above, starting with primary antibody incubation.

Immunofluorescence Staining

NIH3T3 Cells—NIH3T3 cells were grown on sterilized glass coverslips in a 6-well plate until about 70% confluence. The cells were rinsed twice in pre-warmed 1× PBS. Cold ~100% methanol was added to the wells and incubated on ice for 10 min. The fixative was removed, and the cells were incubated in TBS-0.5% Triton X-100 for 10 min. The cells were then rinsed in three changes of TBS-0.1% Triton X-100, then blocked in 3% BSA in TBS-0.1% Triton X-100 for 30 min-1hr at RT, then incubated with primary antibodies diluted in 3% BSA solution, for 1-2hrs at RT with shaking, then rinsed 3× 5 min in TBS-0.1% Triton X-100. The secondary antibodies diluted in 3% BSA solution were then added, and incubated for 1-2 hrs at RT with shaking. The cells were finally rinsed 3× 5 min in TBS-0.1% Triton X-100, then each coverslip was drained and mounted onto a microscope slide with a drop of mounting medium containing DAPI, then sealed with nail varnish.

Mouse Oocytes—To stain for anillin and septin 11 in meiosis I, the oocytes were collected as described above and cultured until the required stage of meiotic maturation. Just before fixation, the zonae pellucidae of oocytes was removed by a brief (2-5 min) treatment in 1% pronase (Sigma) diluted in M2 medium, and pre-warmed to 37°C. The oocytes were rinsed in several drops of M2 medium without pronase and cultured in M16 in the incubator to recover for 30 min before fixation. After recovery, the oocytes were quickly dropped into a well containing pre-chilled ~100% methanol, and incubated at -20°C for 5 min. The oocytes were then collected and put in 0.25% Triton X-100 in TBS and incubated for 20 min at RT with shaking, then transferred to a well containing 3% BSA in TBS-0.1% Triton X-100, and blocked for 30 min at RT. The oocytes were then incubated with the primary antibodies diluted in blocking solution, overnight at 4°C, in a humidified container. A set of 3× 5 min washes in blocking solution was carried out before incubation with the secondary antibodies diluted in blocking buffer, for 1-2hrs at RT. The wash set was repeated, and the oocytes were affixed onto poly-L-Lysine coated round 12mm coverslips (BD BioCoat) and mounted onto a microscope slide with a drop of mounting medium containing DAPI, then sealed with nail varnish.

Mouse oocytes in meiosis II were fixed in either one of two formaldehyde-containing buffers: 1) 80 mM K-PIPES, pH 6.8, 1mM MgCl2, 10 mM EGTA, 0.1% Triton X-100 and 4% formaldehyde (Straight et al., 2003); 2) 100 mM HEPES, pH 7.0, 50 mM EGTA, 10 mM MgSO4, 2% formaldehyde and 0.2% Triton X-100 (Schuh and Ellenberg, 2008). The oocytes were fixed in pre-warmed fixation buffer for 20 minutes at 37°C, permeabilized in 0.25% Triton X-100 in PBS for 20 minutes at RT, blocked in 3% BSA in PBS with 0.1% Triton X-100 for 30 min at RT, then incubated in primary antibodies diluted in blocking solution, overnight at 4°C. Washes and secondary antibody incubations were carried out as described above for cold methanol fixation.

Antibodies

Three anillin antibodies (one kindly provided by Alisa Piekny, and two antibodies produced at the IRIC Proteomics facility for the Maddox lab) were tested by Western blotting on murine cell extracts as described above. The following antibodies were used for this work: Rabbit anti anillin G3165 (antigen: mouse ANLN amino acids 252-367) at 1:100; FITC-

conjugated α-tubulin (Sigma) at 1:50; Alexa Fluor 546 goat anti-rabbit (Molecular Probes/Life Technologies) at 1:100; Rabbit anti non-muscle myosin IIA (Sigma) at 1:100 (for Western blot); Rabbit anti non-muscle myosin IIA (Covance) at 1:100; Alexa Fluor 647 Phalloidin (Molecular Probes/Life Technologies). Myosin IIA was chosen as a co-stain for the meiotic cytokinetic ring, whereas myosin IIB (not studied here) localizes to a cap above the meiotic spindle (Deng et al., 2007; Simerly et al., 1998). DAPI stain for DNA was added to the mounting medium.

Data Analysis

Real time PCR data was analyzed as described (Pfaffl, 2001). Quantification of Western blots was performed with ImageJ. Immunofluorescence images were analysed with Imaris software and ImageJ. Images were further processed with ImageJ and Adobe Photoshop. All figures were prepared in Adobe InDesign and Adobe Illustrator.

Acknowledgments

We thank Yojiro Yamanaka for thoughtful reading of this manuscript, and the Meloche lab (IRIC), Alisa Piekny (Concordia University) and William Trimble (SickKids Hospital) for reagents. This work was supported by GM102390 from the NIH to ASM.

References

Argiros H, Henson L, Holguin C, Foe V, Shuster CB. Centralspindlin and chromosomal passenger complex behavior during normal and Rappaport furrow specification in echinoderm embryos. Cytoskeleton. 2012; 69:840–853.10.1002/cm.21061 [PubMed: 22887753]

Azoury J, Lee KW, Georget V, Hikal P, Verlhac MH. Symmetry breaking in mouse oocytes requires transient F-actin meshwork destabilization. Dev Camb Engl. 2011; 138:2903–2908.10.1242/dev.060269

Azoury J, Lee KW, Georget V, Rassinier P, Leader B, Verlhac MH. Spindle Positioning in Mouse Oocytes Relies on a Dynamic Meshwork of Actin Filaments. Curr Biol. 2008; 18:1514–1519.10.1016/j.cub.2008.08.044 [PubMed: 18848445]

Behringer, R. Manipulating the mouse embryo: a laboratory manual. Fourth. Cold Spring Harbor Laboratory Press; Cold Spring Harbor, New York: 2014.

Bringmann H. Mechanical and genetic separation of aster- and midzone-positioned cytokinesis. Biochem Soc Trans. 2008; 36:381.10.1042/BST0360381 [PubMed: 18481963]

Chaigne A, Verlhac MH, Terret ME. Spindle positioning in mammalian oocytes. Exp Cell Res. 2012; 318:1442–1447.10.1016/j.yexcr.2012.02.019 [PubMed: 22406266]

Cowan C. Ran and Rac in Mouse Eggs: Cortical Polarity and Spindle Positioning. Dev Cell. 2007; 12:174–176.10.1016/j.devcel.2007.01.007 [PubMed: 17276334]

D'Avino PP, Takeda T, Capalbo L, Zhang W, Lilley KS, Laue ED, Glover DM. Interaction between Anillin and RacGAP50C connects the actomyosin contractile ring with spindle microtubules at the cell division site. J Cell Sci. 2008; 121:1151–1158.10.1242/jcs.026716 [PubMed: 18349071]

Dehapiot B, Carrière V, Carroll J, Halet G. Polarized Cdc42 activation promotes polar body protrusion and asymmetric division in mouse oocytes. Dev Biol. 2013; 377:202–212.10.1016/j.ydbio.2013.01.029 [PubMed: 23384564]

Deng M, Suraneni P, Schultz RM, Li R. The Ran GTPase Mediates Chromatin Signaling to Control Cortical Polarity during Polar Body Extrusion in Mouse Oocytes. Dev Cell. 2007; 12:301–308.10.1016/j.devcel.2006.11.008 [PubMed: 17276346]

Dorn JF, Zhang L, Paradis V, Edoh-Bedi D, Jusu S, Maddox PS, Maddox AS. Actomyosin Tube Formation in Polar Body Cytokinesis Requires Anillin in C. elegans. Curr Biol. 2010; 20:2046–2051.10.1016/j.cub.2010.10.030 [PubMed: 21055941]

Ducibella T, Kurasawa S, Rangarajan S, Kopf GS, Schultz RM. Precocious loss of cortical granules during mouse oocyte meiotic maturation and correlation with an egg-induced modification of the zona pellucida. Dev Biol. 1990; 137:46–55. [PubMed: 2104813]

Duncan FE, Moss SB, Schultz RM, Williams CJ. PAR-3 defines a central subdomain of the cortical actin cap in mouse eggs. Dev Biol. 2005; 280:38–47.10.1016/j.ydbio.2004.12.034 [PubMed: 15766746]

Estey MP, Di Ciano-Oliveira C, Froese CD, Bejide MT, Trimble WS. Distinct roles of septins in cytokinesis: SEPT9 mediates midbody abscission. J Cell Biol. 2010; 191:741–749.10.1083/jcb.201006031 [PubMed: 21059847]

Field CM, Alberts BM. Anillin, a contractile ring protein that cycles from the nucleus to the cell cortex. J Cell Biol. 1995; 131:165–178. [PubMed: 7559773]

Field CM, Coughlin M, Doberstein S, Marty T, Sullivan W. Characterization of anillin mutants reveals essential roles in septin localization and plasma membrane integrity. Dev Camb Engl. 2005; 132:2849–2860.10.1242/dev.01843

Frenette P, Haines E, Loloyan M, Kinal M, Pakarian P, Piekny A. An Anillin-Ect2 Complex Stabilizes Central Spindle Microtubules at the Cortex during Cytokinesis. PLoS ONE. 2012; 7:e34888.10.1371/journal.pone.0034888 [PubMed: 22514687]

Fung, KYY.; Dai, L.; Trimble, WS. International Review of Cell and Molecular Biology. Elsevier; 2014. Cell and Molecular Biology of Septins; p. 289-339.

Giansanti MG, Bonaccorsi S, Gatti M. The role of anillin in meiotic cytokinesis of Drosophila males. J Cell Sci. 1999; 112:2323–2334. [PubMed: 10381388]

Green RA, Paluch E, Oegema K. Cytokinesis in animal cells. Annu Rev Cell Dev Biol. 2012; 28:29–58.10.1146/annurev-cellbio-101011-155718 [PubMed: 22804577]

Gregory SL, Ebrahimi S, Milverton J, Jones WM, Bejsovec A, Saint R. Cell Division Requires a Direct Link between Microtubule-Bound RacGAP and Anillin in the Contractile Ring. Curr Biol. 2008; 18:25–29.10.1016/j.cub.2007.11.050 [PubMed: 18158242]

Halet G, Carroll J. Rac Activity Is Polarized and Regulates Meiotic Spindle Stability and Anchoring in Mammalian Oocytes. Dev Cell. 2007; 12:309–317.10.1016/j.devcel.2006.12.010 [PubMed: 17276347]

Hickson GRX, O'Farrell PH. Anillin: a pivotal organizer of the cytokinetic machinery. Biochem Soc Trans. 2008; 36:439.10.1042/BST0360439 [PubMed: 18481976]

Hickson GRX, O'Farrell PH. Rho-dependent control of anillin behavior during cytokinesis. J Cell Biol. 2008; 180:285–294.10.1083/jcb.200709005 [PubMed: 18209105]

Huang YW, Yan M, Collins RF, DiCiccio JE, Grinstein S, Trimble WS. Mammalian septins are required for phagosome formation. Mol Biol Cell. 2008; 19:1717–1726. [PubMed: 18272790]

Kechad A, Jananji S, Ruella Y, Hickson GRX. Anillin Acts as a Bifunctional Linker Coordinating Midbody Ring Biogenesis during Cytokinesis. Curr Biol. 2012; 22:197–203.10.1016/j.cub.2011.11.062 [PubMed: 22226749]

Kinoshita M, Field CM, Coughlin ML, Straight AF, Mitchison TJ. Self- and actin-templated assembly of mammalian septins. Dev Cell. 2002; 3:791–802. [PubMed: 12479805]

Leader B, Lim H, Carabatsos MJ, Harrington A, Ecsedy J, Pellman D, Maas R, Leder P. Formin-2, polyploidy, hypofertility and positioning of the meiotic spindle in mouse oocytes. Nat Cell Biol. 2002; 4:921–928.10.1038/ncb880 [PubMed: 12447394]

Liu J, Fairn GD, Ceccarelli DF, Sicheri F, Wilde A. Cleavage Furrow Organization Requires PIP2-Mediated Recruitment of Anillin. Curr Biol. 2012; 22:64–69.10.1016/j.cub.2011.11.040 [PubMed: 22197245]

Longo FJ, Chen DY. Development of cortical polarity in mouse eggs: involvement of the meiotic apparatus. Dev Biol. 1985; 107:382–394. [PubMed: 4038667]

Lukoyanova N, Baldwin SA, Trinick J. 3D Reconstruction of Mammalian Septin Filaments. J Mol Biol. 2008; 376:1–7.10.1016/j.jmb.2007.11.029 [PubMed: 18083193]

Maddox AS, Azoury J, Dumont J. Polar body cytokinesis. Cytoskeleton. 2012; 69:855–868. [PubMed: 22927361]

Maddox AS, Habermann B, Desai A, Oegema K. Distinct roles for two C. elegans anillins in the gonad and early embryo. Development. 2005; 132:2837–2848.10.1242/dev.01828 [PubMed: 15930113]

Mostowy S, Cossart P. Septins: the fourth component of the cytoskeleton. Nat Rev Mol Cell Biol. 201210.1038/nrm3284

Na J, Zernicka-Goetz M. Asymmetric Positioning and Organization of the Meiotic Spindle of Mouse Oocytes Requires CDC42 Function. Curr Biol. 2006; 16:1249–1254.10.1016/j.cub.2006.05.023 [PubMed: 16782018]

Oegema K, Savoian MS, Mitchison TJ, Field CM. Functional analysis of a human homologue of the Drosophila actin binding protein anillin suggests a role in cytokinesis. J Cell Biol. 2000; 150:539–552. [PubMed: 10931866]

Paolo D'Avino P. How to scaffold the contractile ring for a safe cytokinesis -lessons from Anillin-related proteins. J Cell Sci. 2009; 122:1071–1079.10.1242/jcs.034785 [PubMed: 19339546]

Pfaffl MW. A new mathematical model for relative quantification in real-time RT-PCR. Nucleic Acids Res. 2001; 29:e45. [PubMed: 11328886]

Piekny AJ, Glotzer M. Anillin Is a Scaffold Protein That Links RhoA, Actin, and Myosin during Cytokinesis. Curr Biol. 2008; 18:30–36.10.1016/j.cub.2007.11.068 [PubMed: 18158243]

Piekny AJ, Maddox AS. The myriad roles of Anillin during cytokinesis. Semin Cell Dev Biol. 2010; 21:881–891.10.1016/j.semcdb.2010.08.002 [PubMed: 20732437]

Schuh M, Ellenberg J. A New Model for Asymmetric Spindle Positioning in Mouse Oocytes. Curr Biol. 2008; 18:1986–1992.10.1016/j.cub.2008.11.022 [PubMed: 19062278]

Simerly C, Nowak G, de Lanerolle P, Schatten G. Differential expression and functions of cortical myosin IIA and IIB isotypes during meiotic maturation, fertilization, and mitosis in mouse oocytes and embryos. Mol Biol Cell. 1998; 9:2509–2525. [PubMed: 9725909]

Steuerwald N, Cohen J, Herrera RJ, Sandalinas M, Brenner CA. Association between spindle assembly checkpoint expression and maternal age in human oocytes. Mol Hum Reprod. 2001; 7:49–55. [PubMed: 11134360]

Straight AF, Cheung A, Limouze J, Chen I, Westwood NJ, Sellers JR, Mitchison TJ. Dissecting temporal and spatial control of cytokinesis with a myosin II Inhibitor. Science. 2003; 299:1743–1747.10.1126/science.1081412 [PubMed: 12637748]

Su YQ, Sugiura K, Woo Y, Wigglesworth K, Kamdar S, Affourtit J, Eppig JJ. Selective degradation of transcripts during meiotic maturation of mouse oocytes. Dev Biol. 2007; 302:104–117. [PubMed: 17022963]

Vinot S, Le T, Maro B, Louvet-Vallée S. Two PAR6 proteins become asymmetrically localized during establishment of polarity in mouse oocytes. Curr Biol. 2004; 14:520–525. [PubMed: 15043819]

Von Dassow G, Verbrugghe KJC, Miller AL, Sider JR, Bement WM. Action at a distance during cytokinesis. J Cell Biol. 2009; 187:831–845.10.1083/jcb.200907090 [PubMed: 20008563]

Wang Q, Racowsky C, Deng M. Mechanism of the chromosome-induced polar body extrusion in mouse eggs. Cell Div. 2011; 6:9. [PubMed: 21492451]

Yi K, Li R. Actin cytoskeleton in cell polarity and asymmetric division during mouse oocyte maturation. Cytoskeleton. 2012; 69:727–737. [PubMed: 22753278]

Yi K, Unruh JR, Deng M, Slaughter BD, Rubinstein B, Li R. Dynamic maintenance of asymmetric meiotic spindle position through Arp2/3-complex-driven cytoplasmic streaming in mouse oocytes. Nat Cell Biol. 2011; 13:1252–1258.10.1038/ncb2320 [PubMed: 21874009]

Highlights

- Anillin protein level increases during mouse oocyte maturation.
- Anillin localizes to a broad ring over anaphase I spindles.
- Anillin localizes to a cortical stripe over the meiosis II spindle midzone.
- Division plane specification may differ between mouse meiosis I and II.

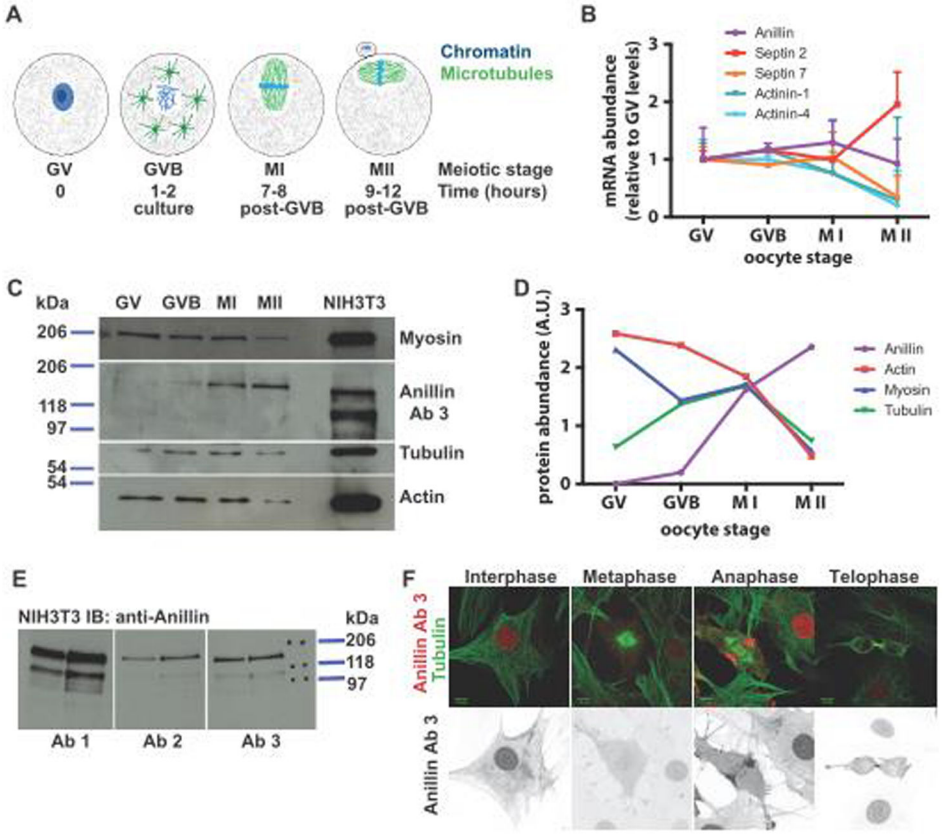

Figure 1. Anillin mRNA and protein expression during meiotic maturation of the mouse oocyte

(A) Schematic representation of meiotic maturation of the mouse oocyte with the different stages indicated and time (in hours) after isolation. GV= germinal vesicle stage; GVB= germinal vesicle breakdown; MI= metaphase I; MII= metaphase II. (B) Chart derived from qRT-PCR data showing transcript levels for each stage of meiotic maturation for the indicated genes. The levels were normalised relative to the GV stage (control) using the Pfaffl equation. (C) Western blot of mouse oocyte extracts prepared from the indicated stages of meiotic maturation and probed for the proteins indicated. NIH3T3 mouse cell line extracts are used as positive control. (D) Quantification of relative protein levels in oocytes from the Western blot shown in (C). (E) Western blot of NIH3T3 cell extracts probed for three different anillin antibodies, separately. Pairs of lanes were loaded with 7 μl or 15 μl of the same extract. (F) Immunofluorescence staining of NIH3T3 cells to localize anillin (red) with tubulin (green) and DNA (blue) at the indicated stages of the mitotic cell cycle.

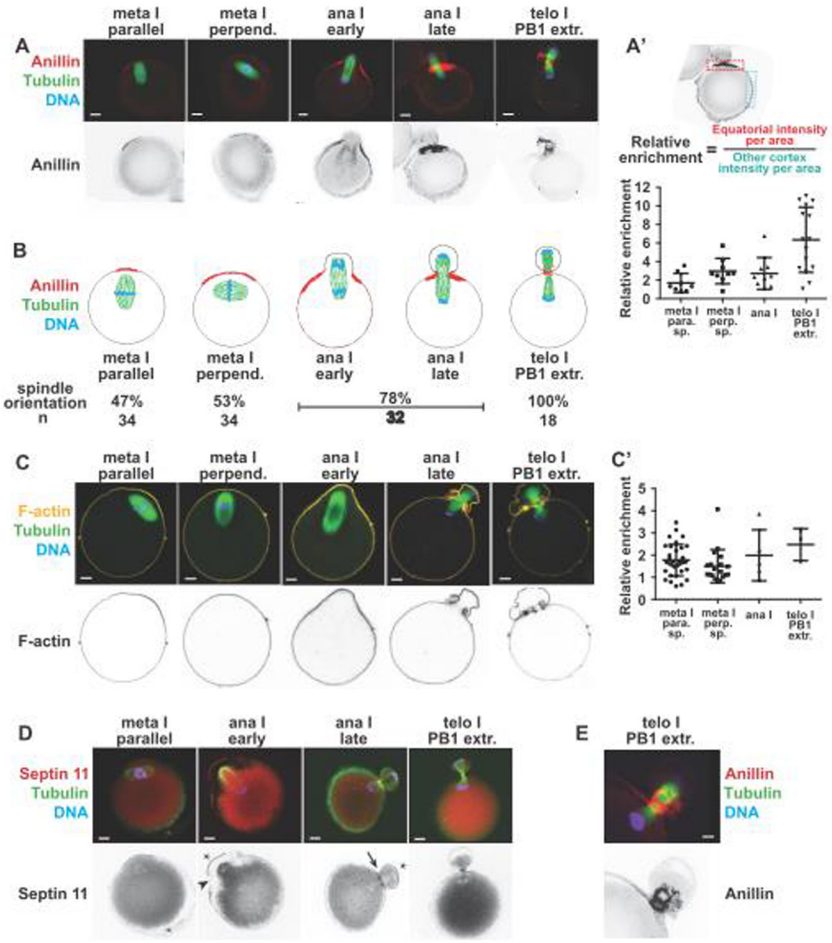

Figure 2.

Anillin, septin 11 and F-actin enrich in the polar cortex of mouse oocytes during the first meiotic division.

(A) The localization of anillin (red) together with tubulin (green) and DNA (blue) in mouse oocytes undergoing meiosis I division. The lower panels show anillin alone. Quantification of anillin enrichment at the cortex is provided (A′) for the meiosis I stages shown in (A). (B) Schematic representation of anillin localization as shown in (A), relative to the first meiotic spindle. The proportion of oocytes showing each of the indicated spindle orientations is given below. (C) The localization of F-actin (yellow) together with tubulin (green) and DNA (blue) in mouse oocytes undergoing meiosis I division. The lower panels show F-actin alone. Quantification of F-actin enrichment at the cortex is provided (C′) for the meiosis I stages shown in (C). (D) The localization of septin 11 (red) together with tubulin (green) and DNA (blue) in mouse oocytes undergoing meiosis I division. The lower panels show septin 11 alone, where it is enriched at the apical cortex of the polar body in early anaphase (asterix), and at the contractile ring in late anaphase (arrow). The arrowhead points to absence of Septin 11 at the early furrow. (E) Anillin localization in a telophase I oocyte showing a two-ring stack, one of which is more closely associated with the polar body while the other is on the oocyte surface. The lower panel shows anillin alone while the top panel

shows anillin (red) together with tubulin (green) and DNA (blue). Scale bars= 10 μm (A-D) and 5 μm (E).

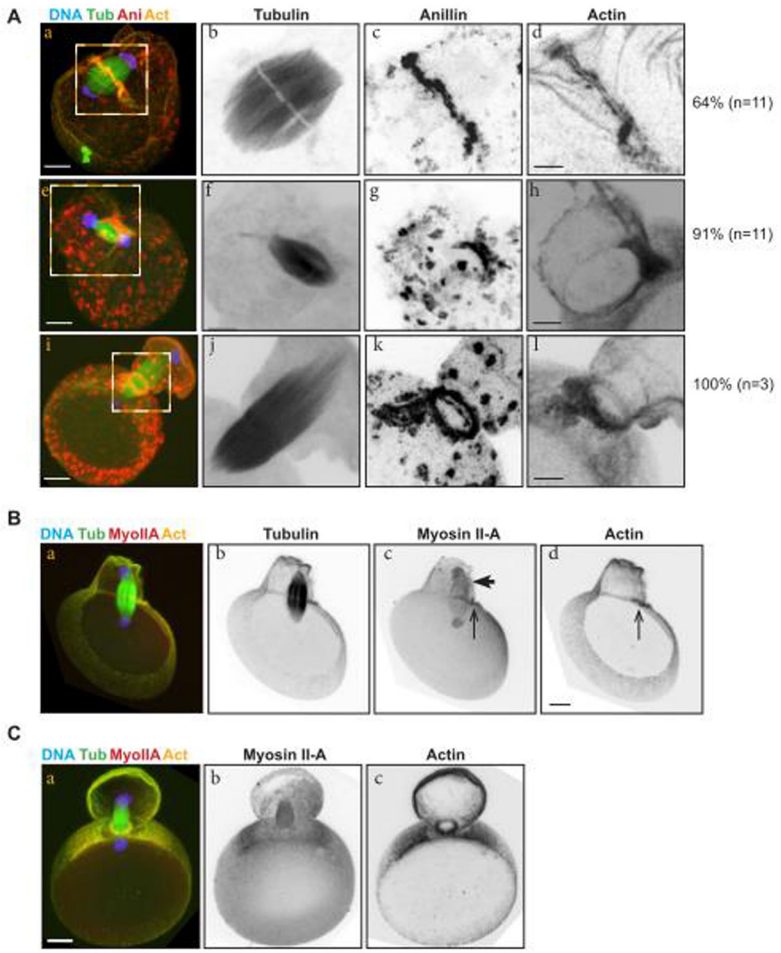

Figure 3.

Anillin and actin form a curvilinear structure over the meiosis II spindle midzone.

(A) Activated mouse eggs undergoing anaphase II before spindle rotation (top row), after spindle rotation (middle row) and in telophase II (bottom row) stained for tubulin (green), anillin (red), F-actin (yellow) and DNA (blue). Right columns are magnifications of the boxed regions in the left column. The proportion of eggs showing the staining patterns is indicated beside the images. Scale bars = 10 μm (left column) and 5 μm (monochrome images). (B) An activated egg in anaphase II, after spindle rotation, showing tubulin, myosin IIA and actin staining. Arrowhead: close association of the extruded spindle half with the lateral cortex of the second polar body; arrow: the cytokinetic furrow coinciding with the spindle midzone. Scale bars = 10 μm. (C) An activated mouse egg in telophase II stained for tubulin, myosin IIA, actin and DNA. Scale bar = 10 μm.

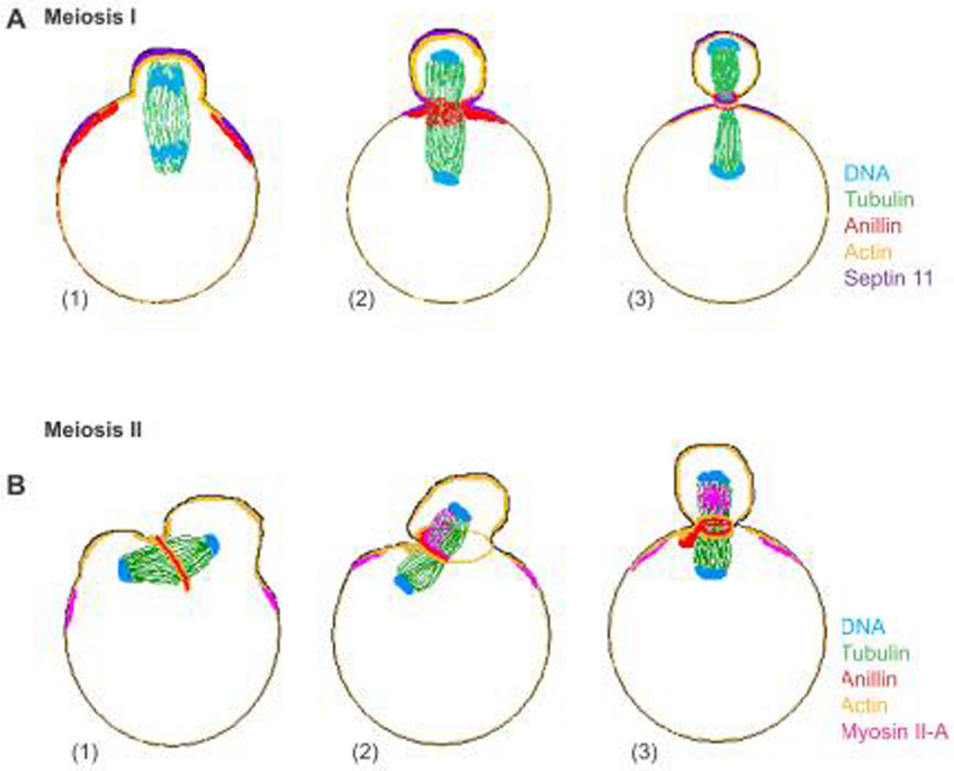

Figure 4.

Distinct mechanisms of division plane specification in mouse oogenic meiosis I and II. Graphical summary depicting anillin localization during meiosis I and II divisions of the mouse oocyte. The numbers indicate the sequence of events as observed in immunolocalization studies: (1) mid anaphase; (2) late anaphase; (3) telophase. Components' localization as determined in this study are represented in colors according to the key at the left.

Table 1

List of Primers for PCR/ Real Time-PCR

Primer name	Primer sequence 5′>3′
β-Actin F	GCTCTTTTCCAGCCTTCCTT
β -Actin R	CGGATGTCAACGTCACACTT
GAPDH F	TGACGTGCCGCCTGGAGAAA
GAPDH R	AGTGTAGCCCAAGATGCCCTT
α-actinin-4 F	GCACCCTTCAACAACTGGAT
α-actinin-4 R	CAGGGTGGACTTGAACTGGT
α-actinin-1 F	CAAGGCCTTGCTCAAGAAG
α-actinin-1 R	ACTTGGCGAGTCATAGTA
Septin-2 F	GAGGTGGAGAACCCAGAACA
Septin-2 R	CAGCCTCCTTTTCAAGCAAG
Septin-7 F	GGTGAATCTGGACTGGGAAA
Septin-7 R	ACTTTGGATTGCTCCACCTG
Anillin F	CAGCTCAAACAGGAACGTGA
Anillin R	CAGAAGTCAATGGGGTGCTT